Original Article

Investigation into the formation of silicate deposits in the steam sterilization process

A. Gassner*, W. Fuchs[1], L. Waidelich[1], H. Mozaffari-Jovein[2]

[1] Aesculap AG, Am Aesculap-Platz, 78532 Tuttlingen, Germany; [2] Hochschule Furtwangen, STW Material-Technologie, 78532 Tuttlingen, Germany

Corresponding author:
Andreas Gassner
STW Material-Technologie
Take-Off Gewerbepark
Haus Nr. 9
78579 Neuhausen ob Eck

andreas.gassner@stw.de

Conflict of interest:
All authors confirm that there is no conflict of interest according to the guidelines of the International Committee of Medical Journal editors (ICMJE).

Summary

The present study investigated the formation and fixation of silicate deposits during steam sterilization. First, transfer of silicic acid from the feed water into the sterilization steam onto the sterile supplies was analysed in theory by comparing the process parameters of all substeps of a typical steam sterilization process with a solubility diagram for silicic acid in water and in steam. Next, in furnace tests silicate deposits were selectively deposited onto test specimen made of non-rusting steel and with instrument-like surfaces. Deposit formation was visualized through digital photography and differential interference contrast (DIC) microscopy. In addition, topography images were obtained with atomic force microscopy (AFM) and the chemical composition of surfaces was determined with X-ray fluorescence analysis. Theoretical considerations supported the notion of a pressure- and temperature-dependent solubility of silicic acid in steam which, based on the steam sterilization process parameters, led to extensive entrainment of silicic acid into, and little removal from, the autoclave. Furthermore, experimental findings demonstrated that entrainment of silicic acid compounds gave rise to high, interlocking silicate margins on the test specimen, with a thin flat configuration within the dried drops. By combining the theoretical considerations and experimental findings, it was possible for the first time to add to the literature repository an explanation for the transfer of silicic acid to the sterile supplies and for the mechanism underling the transformation into visible deposits.

Keywords
- steam sterilization
- silicate deposits
- silicic acid
- medical instruments/devices

1 Introduction

Reusable surgical instruments are subjected to the most diverse types of stress during the instrument cycle which can manifest on the non-rusting steel used here as surface changes, such as corrosion or discolorations [1]. Silicate deposits are one type of discolorations commonly observed in the field of application. These are seen as drop-shaped layers, like icing, on the instrument surfaces and, since they have a layer thickness of 40 nanometer, can be identified as interference phenomena with a golden brown to violet blue colour [2, 3]. The chemical structure of the deposits corresponds to that of an amorphous silica glass network which has been demonstrated to present no immediate risk to the patient due to its inorganic nature and limited chemical reactivity [2]. Nonetheless, these manifestations time and again result in unfounded hygiene alerts with closure of entire Central Sterile Supply Departments (CSSDs) and operation cancellations [4]. Since silicate deposits additionally obscure visibility of genuinely critical surface changes, thus hampering routine control for batch release, every effort should be made to prevent them [3].

The formation of silicate deposits on surgical instruments during reprocessing is, in addition to the use or entrainment of silicate-based detergents, largely due to silicic acid breakthrough during treatment of the feed water used for steam sterilization [5]. The oxoacids of silicon are known as silicic acid; their parent compound is formed as monosilicic acid through the dissolution of feldspar or amor-

Citation:
Gassner A, Fuchs W, Waidelich L, Mozaffari-Jovein H. Investigation into the formation of silicate deposits in the steam sterilization process. Zentr Steril 2019; 27 (6): 380–386

Manuscript data:
Submitted 18 September 2019
Revised version accepted: 24 October 2019

phous silicon dioxide in water [5]. Under normal conditions at 25°C and 1 bar atmospheric pressure up to 120 mg/l monosilicic acid dissolves in water, whereby the solubility limit varies greatly in accordance with the pH value, pressure and temperature [6]. To avoid silicate deposits during sterilization, EN 285 recommends a feed water silicic acid content of less than 1.0 mg/l [7]. To assure the required limit value, the process water is treated by conveying it first through a cation and anion exchanger as well as, in most cases, through a reverse osmosis system and then the water conductivity is measured with respect to its purity. However, one problem encountered here is that only above a pH value of 8.5 does silicic acid appreciably dissociate in the ionogenic state and under typical reprocessing conditions thus does not contribute to the conductivity of the feed water [8]. This means that what is perceived as a good water quality with low conductivity may contain a high silicic acid content which can be later carried over into the sterilization steam and deposited on the surgical instruments.

As such, the appearance and structure of silicate deposits have been analysed in greater detail and reported in the literature. Furthermore, their trigger in the form of silicic acid as well as their origin and entrainment to the steam sterilization feed water have been described. But, to date, no link has been established between these. Hence, no explanation has been given for the transfer of silicic acid into the sterilization steam, its deposition on the sterile supplies following condensation or for its mechanism of conversion to silicate deposits.

The aim of the present study was therefore to explore the theoretical considerations regarding the behaviour of silicic acid acid compounds from their carryover from the sterilization steam to their deposition on the instruments and, by combining these insights with experimental studies, to formulate a mechanism explaining the formation and fixation of silicate deposits. In this study a feed water silicic acid content well above the recommended limit value was used since that worst case scenario was deemed highly likely to lead to the formation of the deposits under investigation.

2 Materials and Methods

2.1 Process analysis

At the start of the study, the transport of silicic acid from the feed water into the sterilization steam and its deposition on the sterile supplies were theoretically analysed. To that effect, the temperature and pressure values typically used for steam sterilization partial processes were applied and, through comparison with a solubility diagram, the maximum amounts of silicic acid in the water and steam were determined. It was thought that this would allow conclusions to be drawn regarding the silicic acid concentrations present and persisting in each process step.

2.2 Experimental studies

The deposition of silicic acid compounds on surgical instruments and their transformation to silicate deposits were explored by means of furnace tests using flat steel samples, with surfaces simulating those of real instruments, and a silicic acid-based test solution.

The baseline material was martensitic, non-rusting steel of type 1.4021 (X20Cr13) as specified in ISO 7153-1 [9] and whose chemical composition is presented in Table 1. From a sheet of that material measuring 3 mm in thickness, test specimen with a length of 90 mm and width of 30 mm were produced by means of shearing. Then the samples were hardened through austenitization in a vacuum furnace at 1025°C, followed by quenching in a nitrogen atmosphere and finally tempering at 280°C. To produce surface conditions reflecting everyday practice as per DIN 96298-3 [10], the samples were subjected to a vibratory finishing process in oxalic acid and neutral water followed by electropolishing at 20 A/dm² and final polish using a three micrometer diamond suspension. Next, one-third of the sample surface was brushed with a 3M Scotch-Brite wheel and a further one-third was rendered matted with glass pearls with a granulation of 40–70 µm at 5 bar jet pressure. The rest of the surface area was covered with a masking tape throughout that time. To finish off, the samples were passivated in citric acid, cleaned with ethanol for 15 minutes in an ultrasonic bath and dried with compressed air.

The aim of the next step was to generate silicate deposits on the newly produced test specimen. To that effect, first of all 9.5 mg of a solid sodium silicon standard from Alfa Aesar was dissolved in one litre of a demineralized and filtered B. Braun Aqua rinse solution, whose composition is given in Table 2. This was used as the test solution. The silicate content of the solution was similar to the concentration normally measured in natural water [6] and allowed for separate analysis of silicic acid deposition. Next, two of the test specimen were placed in a heat treatment furnace with a temperature of 134°C, manufacturer Nabertherm, make N11/HR, and left for 20 minutes to reach the required temperature. The temperature selected was intended to simulate that of the supplies in an autoclave at the beginning of the drying phase. Humidity simulation was omitted because the aim was to assure the fastest possible removal of water. Once heated, the fur-

Table 1: Chemical composition of non-rusting steel type 1.4021

Elements in normalized mass percent						
C	Cr	Mn	Si	P	S	Fe
0.22	12.90	0.43	0.156	0.01	< 0.0005	Balance

Table 2: Composion of the demineralized and filtered B.Braun Aqua rinse solution

Conductivity	Chloride content	Nitrate content	Sulfate content	Ammonium content	Silicic acid content
≤ 5 µS/cm	≤ 0.5 ppm	≤ 0.2 ppm	≤ 0.2 ppm	≤ 0.2 ppm	≤ 0.2 mg/l

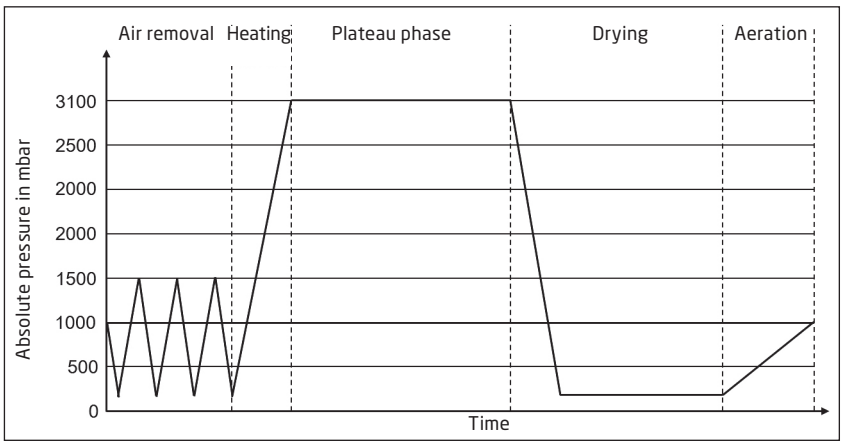

Fig. 1: Schematic diagram of a classic steam sterilization process with fractionated pre-vacuum [7]

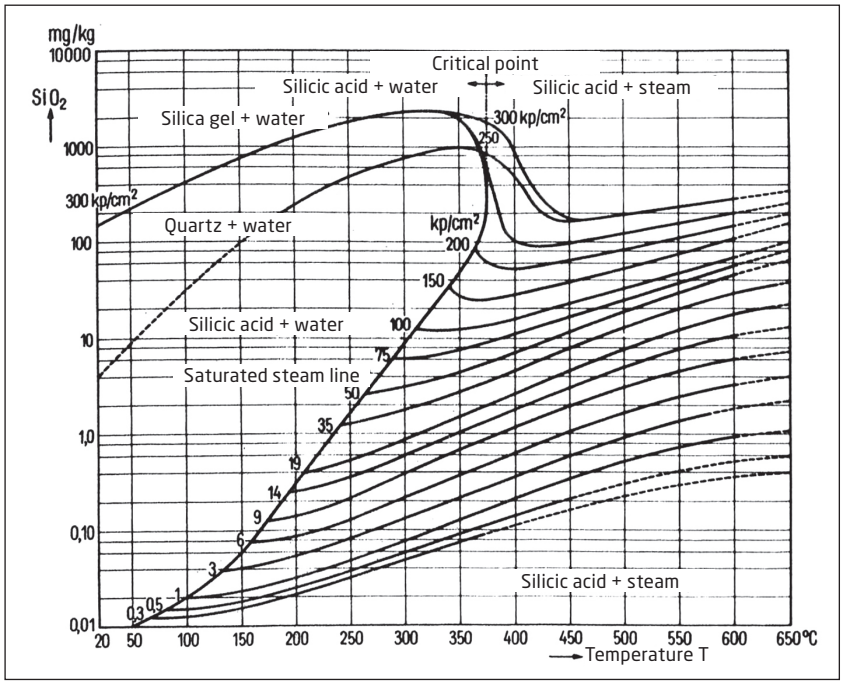

Fig. 2: Solubility diagram of silicic acid in water and steam [11]

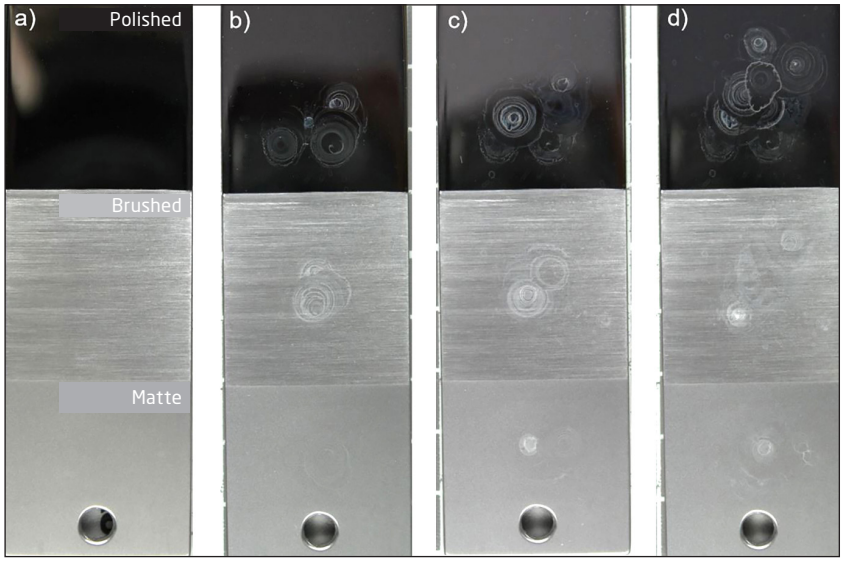

Fig. 3: Digital photographs of flat steel samples. a) 0 cycles, b) 5 cycles, c) 10 cycles, d) 15 cycles

nace was opened and a 15 µl drop of the test solution was applied to the middle of each surface of one test specimen in 15 cycles every 10 minutes. The other test specimen was left untreated to serve as a control (reference).

To observe progressive deposit formation photos were taken with a Canon EOS 500D digital camera of the treated test specimen every five cycles. The remaining characterization was carried out for the surfaces of the untreated and of the test specimen to which the test solution was applied in 15 cycles. The chemical composition of the reference close to the surface, as well as that of the treated sample, was determined with an X-ray fluorescence analyser, make Ametek Spectro Midex, using an acceleration voltage of 45 keV and current of 0.3 mA. Whenever possible the measuring points were situated at the deposits. The thin and, in some cases, transparent layers were visualized using high magnification differential interference contrast (DIC) microscopy, make Keyence VHX-5000, immediately after and one day after application. Finally, contactless determination of the three-dimensional layer formation was undertaken by measuring it with an atomic force microscope (AFM) from the manufacturer Park System, model NX10, using a metallic cantilever.

3 Results

3.1 Process analysis

Comparison of a typical steam sterilization cycle with pre-vacuum phases as illustrated in the schematic diagram in Figure 1 and the solubility diagram for silicic acid in water and steam presented in Figure 2 gives an insight into the potential silicic acid concentration in the individual partial processes. At the start of sterilization, the air is removed from the autoclave chamber through repeated exchanges of vacuum and saturated steam supply. The saturated steam generated from the feed water in the steam generator has a pressure of between 2.05 and 3.1 bar and a temperature of 121 to 134°C. For these parameters a silicic acid content of around 0.05 mg/kg can be determined along the saturated steam line in the solubility diagram. By contrast, in the subsequent vacuum and associated pressure of only around 50 mbar and evaporation temperature of 30°C, a silicic acid concentration of around 0.01 mg/kg is possible in the steam. During

the ensuing heating and plateau phase, saturated steam is reintroduced into the autoclave, whereby the solubility of the silicic acid can be set to a value of 0.05 mg/kg. The ensuing drying phase operates with a new vacuum and generates in the solubility diagram a silicic acid content of 0.01 mg/kg. The process is terminated with aeration and supply of fresh air to the autoclave, which is not substantial in terms of its impact on silicic acid solubility. Besides, the solubility of silicic acid in condensate must be mentioned, which as stated above may reach a value of up to 120 mg/l under normal conditions

3.2 Experimental studies

Figure 3 shows the overview photos of the flat samples with the polished, brushed and matted surfaces following different cycles of test solution application. Here, the polished areas appear dark due to the high light reflection in the camera image, whereas the brushed and matted sections show oriented reflection and a matted appearance, respectively. Immediately after application of five drops, rounded, interlocking white margins can be identified on all surfaces. These are not interconnected and are directed inwards towards the middle of the drop. The margins on the polished surface are spread across a larger surface area, whereas on the brushed and matted sections they are seen at the centre covering a smaller area. The aspects described can also be observed after 10 and 15 application cycles, albeit here some of the margins do not have a rounded shape and are spread across a larger surface area in all surface states. After 15 drop application cycles, a temporal relationship was discernible for the margin configurations. Their white colour changed within a few hours to a light brownish colour. Onset of that effect can be recognized from the polished surface.

The chemical composition of the surface of the reference and of the treated sample is illustrated in Table 3. The polished and brushed reference has a silicon content of around 0.35 %, whereas the matted reference has a silicon content of around 0.5 %. Compared with the reference, the silicon content measured on the deposits after 15 cycles on all surface states had doubled.

Magnified DIC images of the deposit formations on the polished surface are illustrated in Figures 4 to 5. Immediately after application, raised areas of bulging can be observed on the otherwise smooth surface, and correspond to the macroscopically visible drop margins. These exhibit along their width, in some cases, crystal-like lamellae and small black punctiform areas that are not interconnected. Furthermore, dispersed between these areas are transparent, shimmering layers, arranged circularly on top of each other on black areas. A difference in the height of these layers is visualized as an iridescent colour. The image changes after sample storage in air for one day. Here, a larger proportion of black bulgings without shimmering layers can be identified. Besides, there is a contrast between the inner and outer region of the drop, whereby a thin flat configuration can be faintly seen within the drop.

A similar picture is seen for the brushed surface images illustrated in Figure 6 and 7. The most conspicuous finding is the oriented roughness following brushing. Besides, black bulgings can be identified along the macroscopic drop margins, interrupted in places. Transparent films can be seen between the margins. However, unlike on the polished surface, the bulgings and layers are no way as clearly visible since a large part of the image information is obscured by the relatively extensive roughness. Within the course of a day the black bulgings become more pronounced against the rough background, while the shimmering layers can no longer be observed. In addition, a contrast can be noted between the inner and outer region of the drop.

The images of the matted surface are shown in Figures 8 to 9. Under magnification the characteristic structure of the surface with its statistically distributed, spherical cavities is visible. Once again, the margins of the deposits exhibit black bulging with transparent films, both of which appear to spread along the cavities. Visibility is greatly obscured by the roughness of the surface. After a day in the air the shimmering layers disappear and are replaced with black bulgings, which now appear

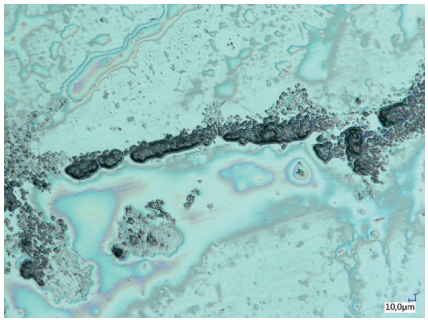

Fig. 4: DIC image of margins – Polished surface immediately after application

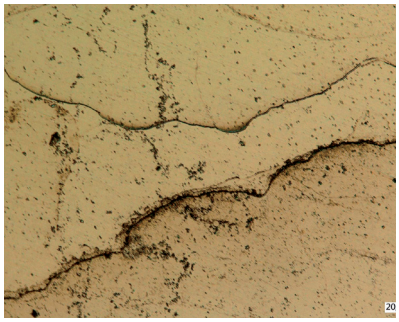

Fig. 5: DIC image of margins – Polished surface after one day

Table 3: Chemical composition of the reference samples and treated test specimen

Flat sample type	Elements in normalized mass percent		
	Si	Cr	Fe
Polished reference	0.37	12.91	83.11
Brushed reference	0.32	12.95	86.73
Matte reference	0.49	13.07	86.44
Polished with silicate	0.78	12.91	82.79
Brushed with silicate	0.65	13.00	86.35
Rendered matte with silicate	0.94	13.04	86.02

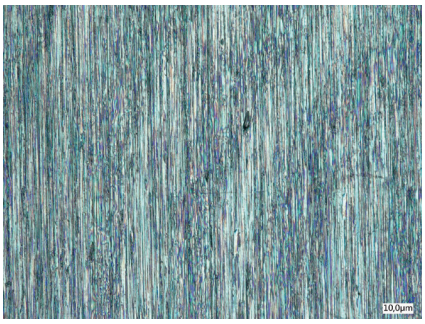

Fig. 6: DIC image of margins – Brushed surface

Fig. 7: DIC image of margins – Brushed surface after one day

Fig. 8: DIC image of margins – Matted surface

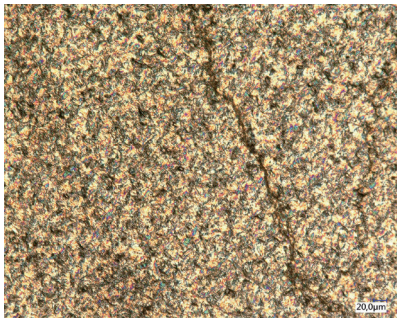

Fig. 9: DIC image of margins – Matted surface after one day

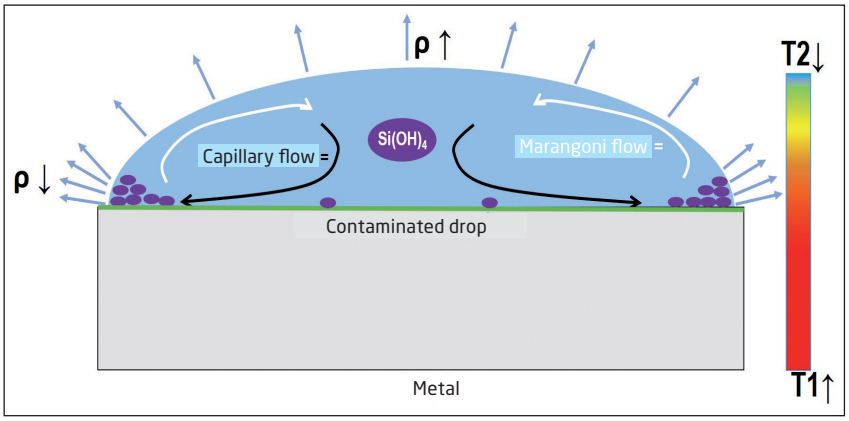

Fig. 13: Schematic diagram of evaporation of a liquid drop and liquid flows generated, transporting silicic acid compounds

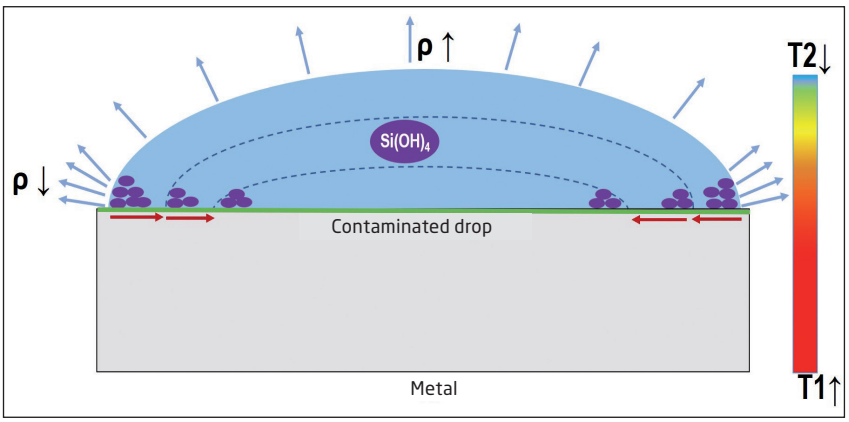

Fig. 14: Schematic evaporation of a liquid drop and displacement of the contact line

to be even more pronounced along the cavities. No contrast can be seen between the inner and outer region of the drop.

The three-dimensional topography of the margins after 24 hours of sample storage is visualized on the atomic force microscopy (AFM) images in Figures 10 to 12. From these can be seen that the margins on all surface states tend to emerge stalk-like from the cavities in the surface, reaching a height of between 200 and 350 nm, and may unite over the cavities in areas of roughness to a width of around 5 µm. In addition, on the polished surface within the former drop a uniform layer measuring 40 nm in thickness can be seen, which as such was not possible to record on the much rougher brushed and matted surfaces.

4 Discussion

Through the combination of theoretical considerations and experimental studies it was possible to formulate a mechanism that may explain the transfer of silicic acid and its transformation to drop-shaped silicate deposits.

Based on the process analysis results, the transfer of silicic acid from the feed water into the autoclave, and its fixation there, has its origin in the variation in pressure and temperature. The saturated steam initially introduced into the autoclave exhibits good solubility for silicic acid, which is why the latter is entrained from the feed water and transported into the sterilization chamber. If the hot steam now comes into contact with the still cold chamber walls and sterile supplies, a silicic acid-based water film is formed over the surfaces through condensation and heats the inside of the autoclave by transmitting energy to it. While part of the water film drips down to the bottom of the chamber and is expelled via the drain from the autoclave, another part is retained as residual water on the chamber walls and instruments. If a vacuum is then generated in the chamber, and at the prevailing negative pressure, water evaporates already at a temperature of around 30 °C. The thermal energy of the hot sterile supplies is enough to slowly convert the residual water to a gaseous state. That is linked to the gradual disintegration of the water film to small drops. However, the problem here is that silicates at

negative pressure can be dissolved only at a very low concentration in the arising steam and therefore persist in the slowly evaporating drops. From that appraisal can be inferred that during the air removal, plateau and drying phases unfolding in the presence of saturated steam, increasingly more silicic acid compounds are transported into the autoclave and, because of the changes in pressure and temperature, they can no longer be transported from the instruments away with the arising steam. That results in considerable transfer of silicic acid to the sterile supplies and its fixation there.

A mechanism for the transformation of the silicic acid compounds to silicate deposits can be postulated on the basis of the behaviour evinced by the water drops on hot surfaces in combination with the experimental findings of this study.

The margins of a water drop on a hot surface are pinned (captured) when evaporating on physical and chemical inhomogeneities determined by the morphology, topography and energy of the material surface. The interface between the drop, material surface and surrounding environment is known as a three-phase contact line [12, 13]. The drop preferentially evaporates from that interface, which is why its volume is reduced. To preserve the contact line water rapidly diffuses in parallel from the inside of the drop to the margin, thus giving rise to capillary flow [14, 15]. Since there are also variations in the temperature and density of the drop, Marangoni flow is generated additionally from the margin into the inside of the drop [16]. The flows thus generated can, in the water drops present in this study, result in transport of the silicic acid compounds to the drop margin where they are fixed because of the capillary forces and thus further concentrated. Besides, a small part of the silicic acid can be deposited uniformly during evaporation within the drop at energy efficient sites. The described procedure is illustrated in Figure 13.

As the volume reduces, so the curvature of the drop increases, raising in turn its surface tension. As from a certain volume, the surface tension is so great that the strength maintaining the contact line is exceeded. That causes inward displacement of the drop margin and another contact line is formed at new energy-efficient inhomogeneities within the drop [16, 17]. However, since the diffusion of the silicic acid compounds is unable to keep pace with this development, they stay behind and form deposits. That process is illustrated in Figure 14.

The areas with deposit formations contain a small amount of water combined with a high silicic acid concentration, which means that the solubility limit of the silicic acid is by far exceeded. Under these conditions, the silicic acid tends to undergo a polycondensation reaction during which individual silicic acid groups may, because of collision processes, form higher-order silicic acid compounds through cleavage of water [5, 6]. If, as in the case described here, water continues to be removed, amorphous silica glass networks can be formed at sites of origin [18]. Such growth mechanisms lead to the formation of the black bulgings and shimmering layers described in this study. Here the black margins indicate networks that have already polycondensed at the drop margin and which, based on the AFM images, have emerged stalk-like at energy-efficient sites such as cavities in areas of roughness and grown in height. By contrast, the shimmering layers point to incompletely condensed silicic acid compounds, which over the course of a few hours cluster together, thus gradually giving rise to networks. Since silicic acid tends to be deposited on already formed networks, the number of black dots may increase, whereas clustering in the shimmering layers serves to explain the formation of thin flat configuration within the drop, which can be seen as contrast on the polished and brushed surfaces. If the proposed mechanism is applied several times, the interlocking drop margins with a demonstrable silicon content and slim flat configuration can be formed, as seen in Figure 3.

The proposed mechanism also permits conclusions to be drawn as regards the silicate deposits with well-delineated drop margins and small flat deposits within the drop, as observed in the instrument cycle. As described above, there is also adhesion of the contact line to chemical surface inhomogeneities, which may include already deposited substances [19, 20]. If silica-based drop margins are formed when silicic acid is first deposited, all subsequent drops will preferably be localized here during sterilization. That is conducive to the further deposition of silicic acid compounds at the same sites and can also result in non-rounded deposits. Furthermore, the bonding strength may increase such that the drop surface tension is able to overcome that only belatedly. Hence, inwards displacement of the contact line is seen only when a very

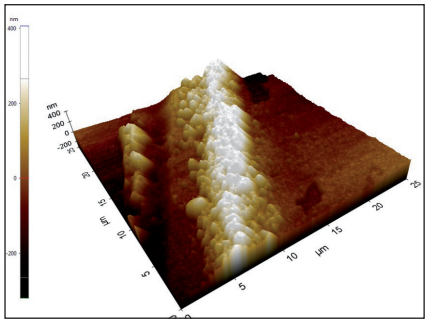

Fig. 10: AFM image of margins – Polished surface after one day

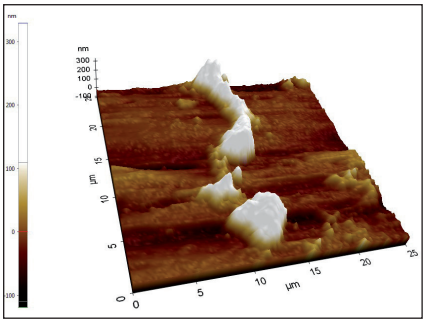

Fig. 11: AFM image of margins – Brushed surface after one day

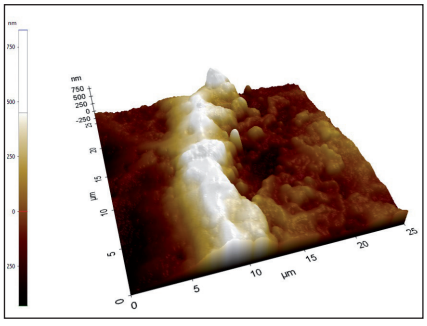

Fig. 12: AFM image of margins – Matted surface after one day

low silicic acid content is present in the drop. That results in continuous preferential deposition at the same drop margin, with only a small proportion within the drop itself. That leads to raised and clearly visible drop margins as well as thin and slightly visible layers within the drop. The colour pattern is due to the interference effects which may become more pronounced or altered after each sterilization cycle.

The influence exerted by the surface is manifested in the visibility of the silicate deposits. Increasing roughness changes the diffusion of light and thus the natural surface sheen. The lower the metal sheen, the more clearly can the sheen of the deposits be noted. That results in increased contrast. In addition, increasing roughness enhances the bonding strength of the water film and can, in turn, result in more residual water on the instruments. This leads to a higher silicic acid content and more growth of silicate deposits. Due to overlapping effects, silicate deposit visibility is greatest in the instrument cycle on matted, and poorest on polished, instrument surfaces.

5 Conclusions

The following conclusions can be drawn from the study presented here:

1. The transfer of silicic acid compounds from the feed water to the sterilization steam and the sterile supplies has its origin in the temperature- and pressure-dependent changes in the solubility of silicic acid in water and steam over the course of steam sterilization.
2. The formation of the classic drop patterns described here is due to the adhesion of evaporating silicic acid-based drops to the hot sterile supplies. The capillary and Marangoni flows generated within the drop preferentially displace the silicic acid compounds to the drop margins, in which they unite to form tall silica glass networks following polycondensation. A small amount of silicic acid is also deposited within the drop, where it may form thin layers.
3. The variability in visibility of silicate deposits on polished, brushed and matted surfaces largely derives from the diffusion of light on rough surfaces, which changes the contrast between the deposits and metal. Variability of the bonding strength is also possible.

6 Take-Home Message

The formation of silicate deposits in the steam sterilization process can be attributed to the pressure- and temperature-dependent solubility of silicic acid in water and steam. This can also result in a high silicic acid content in the sterilization steam and condensate, which cannot be removed during drying and thus persists on the sterile supplies. In the evaporating drop transport mechanisms are activated that displace the silicic acid to the margins, where they are concentrated and give rise to tall structures. At the same time, a thin flat configuration is formed within the drop. As described here, this results in drop-shaped, golden brown to violet blue silicate deposits whose visibility increases, because of the contrast between the deposit and metal, from polished through brushed to matted surfaces. Since the origin of the deposits can be directly linked to silicic acid transport, the only remedial action possible is to minimize the silicic acid content in the feed water through a stable water treatment process. Otherwise, already formed deposits can be removed only by using acidic detergents or through mechanical reworking at the time of repair.

References

1 Wismer, G., Zanette, T.: Handbuch Sterilisation – Von der Reinigung bis zur Bereitstellung von Medizinprodukten, 6. Ausgabe, Wiesbaden: mhp Verlag, 2016:58–83.
2 Tschoerner, M.: Silikatbeläge bei der maschinellen Aufbereitung. Zentr Steril 2012; Suppl. DGSV-Kongress: 18.
3 Arbeitskreis Instrumenten-Aufbereitung: Instrumenten Aufbereitung – Instrumente werterhaltend aufbereiten, Broschüre, 11. Ausgabe, Gütersloh 2017
4 Arbeitskreis Instrumenten-Aufbereitung: Stellungnahme des AKI zu Silikatbelägen auf Instrumentarium – Aussetzung von OPs eine Überreaktion, Presseinformation, http://www.a-k-i.org/aktuelle-themen/veroeffentlichungen/, Möhrfelden-Walldorf, 2011
5 Holleman, A. F, Wiberg, E., Wiberg, N.: Das Silicium, In: Lehrbuch der Anorganischen Chemie, 102 Auflage, Berlin: Gruyter-Verlag, 2007:995–1002.
6 Pohling, R.: Kieselsäure (Silicate, Silicium), In: Chemische Reaktionen in der Wasseranalyse, Springer-Verlag, Berlin Heidelberg, 2015:161–168.
7 DIN EN 285: Sterilisation – Dampf Sterilisatoren – Groß-Sterilisatoren, Juni 2016
8 Stöber, W.: Über die Löslichkeit und das Lösungsgleichgewicht von Kieselsäuren, Colloid and Polymer Science, 1956;147:131–141.
9 DIN EN ISO 7153-1: Chirurgische Instrumente – Werkstoffe – Teil 1: Metalle, Februar 2017
10 DIN 96298-3: Medizinische Instrumente – Begriffe, Messmethoden und Prüfungen, Teil 3: Prüfungen, Oktober 2017
11 Heitmann, H. G.: Die Löslichkeit von Kieselsäure in Wasser und Wasserdampf sowie ihr Einfluß auf Turbinenverkieselungen, Dissertation, Karlsruhe 1963
12 Butt, H. J., Graf, K., Kappl, M.: Physics and Chemistry of Interfaces, 3. Ausgabe, Weinheim: Wiley-VCH Verlag, 2013:143–179.
13 De Gennes, P.G., Brochard-Wyart, F., Quéré, D.: Capillarity and Wetting Phenomena – Drops, Bubbles, Pearls, Waves, New-York: Springer-Verlag, 2002:15–150.
14 Deegan, R. D., Bakajin, O., Dupont, T. F., Huber, G., Nagel, S., Witten, T. A.: Capillary flow as the cause of ring stains from dried liquid drops, Nature International journal of science, 1997; 389: 827–829.
15 Deegan, R. D., Bakajin, O., Dupont, T. F., Huber, G., Nagel, S., Witten, T. A.: Contact line deposits in evaporation drop, Pysical Review Journal, 2000; 62: 756–765.
16 Larson, R. G.: Transport and Deposition Patterns in Drying Sessile Droplets, American Institute of Chemical Engineers Journal, 2014; 60: 1538–1571.
17 Sefiane, K.: Patterns from drying Drops, Advances in Colloid and Interface Science, 2014; 206: 372–381.
18 Heitmann, H. G.: Chemie und Korrosion in Kraftwerken, Essen: Vulkan-Verlag, 2000: 27–179.
19 Yang, X. F.: Equilibrium contact angle and intrinsic wetting hysteresis, Applied Physics Letters, 1995; 67: 2249–2251.
20 Extrand, C. W.: A Thermodynamic Model for Contact Angle Hysteresis, Journal of Colloid and Interface Science, 1998; 207: 11–19.

Translation: Sarah Venkata
sarvenkata@aol.com